
A Study of Posterior Stability for Time-Series Latent Diffusion

Yangming Li, Mihaela van der Schaar
Department of Applied Mathematics and Theoretical Physics
University of Cambridge
y1874@cam.ac.uk

Abstract

Latent diffusion has shown promising results in image generation and permits efficient sampling. However, this framework might suffer from the problem of *posterior collapse* when applied to time series. In this paper, we conduct an impact analysis of this problem. With a theoretical insight, we first explain that posterior collapse reduces latent diffusion to a VAE, making it *less expressive*. Then, we introduce the notion of *dependency measures*, showing that the latent variable sampled from the diffusion model loses control of the generation process in this situation and that latent diffusion exhibits *dependency illusion* in the case of shuffled time series. We also analyze the causes of posterior collapse and introduce a new framework based on this analysis, which addresses the problem and supports a more expressive prior distribution. Our experiments on various real-world time-series datasets demonstrate that our new model maintains a stable posterior and outperforms the baselines in time series generation.

1 Introduction

Latent diffusion [1] has achieved promising performance in image generation and enjoys more efficient sampling than standard diffusion models [2]. However, we argue that this framework might suffer from *posterior collapse* [3] when applied to time series data. This problem mainly occurs in autoencoders [4] for sequence data, where the latent variable becomes uninformative about the data. As a result, the autoregressive decoder tends to ignore it during conditional generation. In this paper, we aim to provide a solid analysis of the negative impacts of posterior collapse on latent diffusion and improve this framework to eliminate the problem.

Impact analysis of posterior collapse. We begin with a theoretical insight to show that a strictly collapsed posterior reduces latent diffusion to a VAE [5], indicating that this problem renders the framework *less expressive*. We then introduce a principled method called *dependency measures*, which quantify the dependencies of an autoregressive decoder on the latent variable and the input partial time series. Through empirical estimation of these measures, we find that the latent variable has an almost exponentially vanishing impact on the decoder during the generation process. An example (i.e., the green bar chart) is shown in the upper left subfigure of Fig. 1. More interestingly, the upper right subfigure illustrates a phenomenon we call *dependency illusion*: the decoder of latent diffusion still heavily relies on input observations (instead of the latent variable) for prediction, even when the time series is randomly shuffled and lacks structural dependencies.

New framework that solves the problem. We start by analyzing the causes of posterior collapse, concluding that it stems from improper framework design and the presence of a *strong decoder* [3]. Building on our analysis, we propose a novel framework that lets the diffusion model and autoencoder interact more effectively than latent diffusion. Specifically, we regard the diffusion process as some

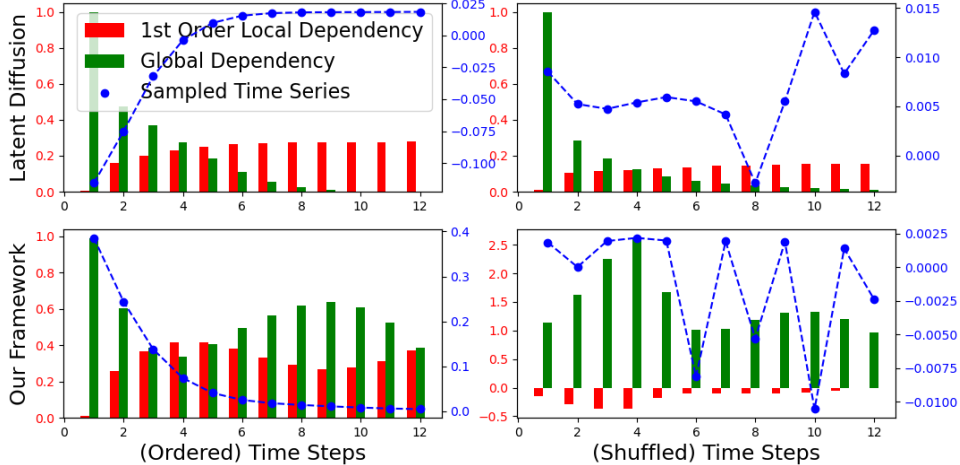


Figure 1: The global and local dependency measures $m_{t,0}, m_{t,t-1}$ (as defined in Sec. 3.2) respectively quantify the impacts of latent variable \mathbf{z} and observation \mathbf{x}_{t-1} on predicting the next one \mathbf{x}_t . We can see that the latent variable \mathbf{z} of latent diffusion loses control of the condition generation $p^{\text{gen}}(\mathbf{X} | \mathbf{z})$, with *dependency illusion* (as introduced in Sec. 3.3) in the case of shuffled time series. In contrast, our framework has no such symptoms of *posterior collapse*.

type of variational inference (with the aim to eliminate the risky KL-divergence regularization and permit an unlimited prior) and apply it to simulate a collapsed posterior (which is to make the decoder sensitive to the latent variable). As shown in the lower two subfigures of Fig.1, our framework exhibits no signs of posterior collapse, such as dependency illusion.

In summary, our paper makes the following contributions:

- We provide a solid impact analysis of *posterior collapse* and introduce *dependency measures*, showing that the problem will reduce latent diffusion to VAE in theory and the latent variable has a vanishing impact on the time series generation in practice;
- We present a new framework that improves the design of time-series latent diffusion. Specifically, our framework gets rid of the risky KL-divergence regularization, permits an expressive prior distribution, and has a sensitive decoder to the latent variable;
- We perform extensive experiments on multiple real-world time-series datasets, showing that our framework has no symptoms of posterior collapse (e.g., *dependency illusion*) and significantly outperforms the baselines in time series generation.

We will publicly release our code upon paper acceptance.

2 Background: Latent Diffusion

The framework of latent diffusion consists of two parts: 1) One of them is a separately trained autoencoder [4] that contains an encoder, mapping high-dimensional or structured data into low-dimensional latent variables; 2) The other is a diffusion model [6] to learn the distribution of latent variables rather than the raw data, which enjoys more efficient computation and better generation quality. For sampling, we first randomly draw a latent variable from the diffusion model, and then apply the decoder of autoencoder to render the variable into a real sample.

Autoencoder. An implementation for the autoencoder is VAE [5]. Let \mathbf{X} and $q^{\text{raw}}(\mathbf{X})$ respectively denote the raw data of any form (e.g., pixel matrix) and its distribution. The encoder \mathbf{f}^{enc} is designed to cast the data \mathbf{X} into a low-dimensional vector $\mathbf{v} = \mathbf{f}^{\text{enc}}(\mathbf{X})$. To get latent variable \mathbf{z} , a reparameterization trick is performed as

$$\begin{cases} \boldsymbol{\mu}, \boldsymbol{\sigma} = \mathbf{W}_\mu \mathbf{v}, \exp(\mathbf{W}_\sigma \mathbf{v}) \\ \mathbf{z} = \boldsymbol{\mu} + \text{diag}(\boldsymbol{\sigma}) \cdot \boldsymbol{\epsilon}, \boldsymbol{\epsilon} \sim \mathcal{N}(\mathbf{0}, \mathbf{I}) \end{cases}, \quad (1)$$

where $\mathbf{W}_\mu, \mathbf{W}_\sigma$ are learnable matrices, and $\text{diag}(\cdot)$ is an operation that casts a vector into a diagonal matrix. The above procedure, which differentially samples a latent variable \mathbf{z} from the posterior $q^{\text{VI}}(\mathbf{z} | \mathbf{X}) = \mathcal{N}(\mathbf{z}; \boldsymbol{\mu}, \text{diag}(\boldsymbol{\sigma}^2))$, is called *variational inference* [7].

The decoder \mathbf{f}^{dec} takes latent variable \mathbf{z} as the input to recover the real sample \mathbf{X} . In VAE, the decoder output $\mathbf{f}^{\text{dec}}(\mathbf{z})$ is used to parameterize a predefined generation distribution $p^{\text{gen}}(\mathbf{X} | \mathbf{z})$. Let sample \mathbf{X} shape as a vector, then an example of distribution $p^{\text{gen}}(\mathbf{X} | \mathbf{z})$ is as $\mathcal{N}(\mathbf{X}; \mathbf{f}^{\text{dec}}(\mathbf{z}), \eta \mathbf{I})$, where scalar η is constant or learnable.

For training, VAE is optimized in terms of the evidence lower bound (ELBO), an upper bound of the exact negative log-likelihood $-\ln \mathbb{E}_{\mathbf{z}}[p^{\text{gen}}(\mathbf{X} | \mathbf{z})]$:

$$\mathcal{L}^{\text{VAE}} = \mathbb{E}_{\mathbf{z} \sim q^{\text{VI}}(\mathbf{z} | \mathbf{X})}[-\ln p^{\text{gen}}(\mathbf{X} | \mathbf{z})] + \text{D}_{\text{KL}}(q^{\text{VI}}(\mathbf{z} | \mathbf{X}) || p^{\text{prior}}(\mathbf{z})), \quad (2)$$

where the prior distribution $p^{\text{prior}}(\mathbf{z})$ is commonly set as a standard Gaussian $\mathcal{N}(\mathbf{0}, \mathbf{I})$. The last term of KL divergence leads the prior $p^{\text{prior}}(\mathbf{z})$ to be compatible with the decoder \mathbf{f}^{dec} for inference, but it is also one cause of *posterior collapse* [3].

Diffusion model. The implementation for the diffusion model is DDPM [2]. The model consists of two Markov chains of $L \in \mathbb{N}^+$ steps. One of them is the diffusion process, which incrementally applies the forward transition kernel,

$$q^{\text{forw}}(\mathbf{z}^i | \mathbf{z}^{i-1}) = \mathcal{N}(\mathbf{z}^i; \sqrt{1 - \beta^i} \mathbf{z}^{i-1}, \beta^i \mathbf{I}), \quad (3)$$

where $\beta^i, i \in [1, L]$ is some predefined variance schedule, to the latent variable $\mathbf{z}^0 := \mathbf{z} \sim q^{\text{latent}}(\mathbf{z})$. Here the distribution of latent variable $q^{\text{latent}}(\mathbf{z})$ is defined as $\int q^{\text{VI}}(\mathbf{z} | \mathbf{X}) q^{\text{raw}}(\mathbf{X}) d\mathbf{X}$. The outcomes of this process are a sequence of new latent variables $\{\mathbf{z}^1, \mathbf{z}^2, \dots, \mathbf{z}^L\}$, with the last one \mathbf{z}^L approximately following a standard Gaussian $\mathcal{N}(\mathbf{0}, \mathbf{I})$ for $L \gg 1$.

The other is the reverse process, which iteratively applies the backward transition kernel,

$$\begin{cases} p^{\text{back}}(\mathbf{z}^{i-1} | \mathbf{z}^i) = \mathcal{N}(\mathbf{z}^{i-1}; \boldsymbol{\mu}^{\text{back}}(\mathbf{z}^i, i), \sigma^i \mathbf{I}) \\ \boldsymbol{\mu}^{\text{back}}(\mathbf{z}^i, i) = \frac{1}{\sqrt{\alpha^i}} \left(\mathbf{z}^i - \beta^i \frac{\boldsymbol{\epsilon}^{\text{back}}(\mathbf{z}^i, i)}{\sqrt{1 - \alpha^i}} \right) \end{cases}, \quad (4)$$

where $\alpha^i = 1 - \beta^i$, $\bar{\alpha}^i = \prod_{k=1}^i \alpha^k$, $\boldsymbol{\epsilon}^{\text{back}}(\cdot)$ is a neural network, and \mathbf{z}^L is an initial sample drawn from $\sim \mathcal{N}(\mathbf{0}, \mathbf{I})$. For the backward variance schedule σ^i , it is commonly set as β^i or $\beta^i(1 - \bar{\alpha}^{i-1})/(1 - \bar{\alpha}^i)$, where $\bar{\alpha}^0 = 0$. The outcome from this process is also a sequence of latent variables $\{\mathbf{z}^{L-1}, \mathbf{z}^{L-2}, \dots, \mathbf{z}^0\}$, where the last variable \mathbf{z}^0 is expected to follow the density distribution of real samples: $q^{\text{latent}}(\mathbf{z}^0)$.

To optimize the diffusion model, common practices adopt a loss function as

$$\mathcal{L}^{\text{DM}} = \mathbb{E}_{i, \mathbf{z}^0, \boldsymbol{\epsilon}}[\|\boldsymbol{\epsilon} - \boldsymbol{\epsilon}^{\text{back}}(\sqrt{\bar{\alpha}^i} \mathbf{z}^0 + \sqrt{1 - \bar{\alpha}^i} \boldsymbol{\epsilon}, i)\|^2], \quad (5)$$

where $\boldsymbol{\epsilon} \sim \mathcal{N}(\mathbf{0}, \mathbf{I})$, $\mathbf{z}^0 \sim q^{\text{latent}}(\mathbf{z}^0)$, and $i \sim \mathcal{U}\{1, L\}$.

3 Problem Analysis

In this section, we first introduce the problem of *posterior collapse*, especially its significance to time-series latent diffusion. Then, we define proper measures that quantify the impact of *posterior collapse* on the models. Finally, we conduct empirical experiments to confirm that time-series diffusion indeed suffers from this problem.

3.1 Definition of Posterior Collapse and Its Impacts

Let us focus on time series $\mathbf{X} = [\mathbf{x}_1, \mathbf{x}_2, \dots, \mathbf{x}_T]$, where every observation $\mathbf{x}_t, t \in [1, T]$ is a D -dimensional vector and T denotes the number of observations. A potential risk of applying the latent diffusion to time series is *posterior collapse* [3], which occurs to some autoencoders [8], especially VAE [9]. A formal definition is as follows.

Problem definition. The posterior of VAE: $q^{\text{VI}}(\mathbf{z} | \mathbf{X})$, is collapsed if it reduces to the Gaussian prior $p^{\text{prior}}(\mathbf{z}) = \mathcal{N}(\mathbf{z}; \mathbf{0}, \mathbf{I})$, irrespective of the conditional \mathbf{X} :

$$q^{\text{VI}}(\mathbf{z} | \mathbf{X}) = p^{\text{prior}}(\mathbf{z}), \forall \mathbf{X} \in \mathbb{R}^{TD}. \quad (6)$$

In this case, the latent variable \mathbf{z} contains no information about conditional \mathbf{X} , otherwise the posterior distribution $q^{\text{VI}}(\mathbf{z} | \mathbf{X})$ would vary depending on different conditionals. Above is also a strict definition. In practice, one is mostly faced with a situation where $q^{\text{VI}}(\mathbf{z} | \mathbf{X}) \approx p^{\text{prior}}(\mathbf{z})$ and it is still proper to claim that posterior collapse happens.

Implications of posterior collapse. A typical and very important symptom of this problem is that the trained decoder \mathbf{f}^{dec} tends to *ignore* the input latent variable \mathbf{z} during the generation process, because the variable \mathbf{z} carries very limited information of time series \mathbf{X} . Obviously, this phenomenon is undesired for conditional generation $p^{\text{gen}}(\mathbf{X} | \mathbf{z})$.

The diffusion model is applied to map a Gaussian noise $\mathbf{z}^L \sim \mathcal{N}(\mathbf{0}, \mathbf{I})$ to latent variable $\mathbf{z}^0 = \mathbf{z}$. For the impact of posterior collapse on that part, we have the below conclusion.

Proposition 3.1 (Gaussian Latent Variables). *For standard latent diffusion, suppose its posterior $q^{\text{VI}}(\mathbf{z} | \mathbf{X})$ is collapsed, then the distribution $q^{\text{latent}}(\mathbf{z})$ of latent variable \mathbf{z} will shape as a standard Gaussian $\mathcal{N}(\mathbf{0}, \mathbf{I})$, which is trivial for the diffusion model to approximate.*

Proof. The proof is fully provided in Appendix A. □

We can see that latent variable \mathbf{z} is just Gaussian in the case of posterior collapse. Therefore, the diffusion model, which is known for approximating complex data distributions [10, 11], is in fact a redundant module in that sense, From another perspective, posterior collapse reduces latent diffusion to VAE, which also samples latent variable \mathbf{z} from a standard Gaussian $\mathcal{N}(\mathbf{0}, \mathbf{I})$. Therefore, we infer that the problem makes latent diffusion *less expressive*.

Takeaway: The problem of *posterior collapse* not only lets the decode \mathbf{f}^{dec} tend to *ignore* the latent variable \mathbf{z} for conditional generation $p^{\text{gen}}(\mathbf{X} | \mathbf{z})$, but also reduces the framework of latent diffusion to VAE, making it *less expressive*.

3.2 Introduction of Dependency Measures

It is very intuitive from above that the problem of *posterior collapse* will make the latent variable \mathbf{z} lose control of the decoder \mathbf{f}^{dec} . To make our claim more solid and confirm that the problem happens to time-series diffusion, we introduce some proper measures that quantify the dependencies of decoder \mathbf{f}^{dec} on various inputs (e.g., variable \mathbf{z}).

Autoregressive decoder. Consider that decoder \mathbf{f}^{dec} has an autoregressive structure, which conditions on latent variable \mathbf{z} and prefix $\mathbf{X}_{1:t-1} = [\mathbf{x}_1, \mathbf{x}_2, \dots, \mathbf{x}_{t-1}]$ to predict the next observation \mathbf{x}_t . With abuse of notation, we set $\mathbf{x}_0 = \mathbf{z}$ and formulate the decoder as

$$\mathbf{h}_t = \mathbf{f}^{\text{dec}}(\mathbf{X}_{0:t-1}), \quad \mathbf{X}_{0:t-1} = [\mathbf{x}_0, \mathbf{x}_1, \mathbf{x}_2, \dots, \mathbf{x}_{t-1}] \quad (7)$$

where the representation $\mathbf{h}_t, t \geq 1$ is linearly projected to multiple parameters (e.g., mean vector and covariance matrix) that determine the distribution $p^{\text{gen}}(\mathbf{x}_t | \mathbf{z}, \mathbf{X}_{1:t-1})$ of some family (e.g., Gaussian). Examples of such a decoder include RNN [12] and Transformer [13]. We put the formulation details of these example in Appendix B.

Dependency measures. The symptom of posterior collapse is that the decoder \mathbf{f}^{dec} heavily relies on prefix $\mathbf{X}_{1:t-1}$ (especially the last observation \mathbf{x}_{t-1}) to compute the representation \mathbf{h}_t , ignoring the guidance of latent variable $\mathbf{x}_0 = \mathbf{z}$. In other words, the variable \mathbf{z} loses control of decoder \mathbf{f}^{dec} in that situation, which is undesired for conditional generation $p^{\text{gen}}(\mathbf{X} | \mathbf{z})$.

Inspired by the technique of integrated gradients [14], we present a new tool: *dependency measures*, which quantify the impacts of latent variable $\mathbf{x}_0 = \mathbf{z}$ and prefix $\mathbf{X}_{1:t-1}$ on decoder \mathbf{f}^{dec} . Specifically, we first set a baseline input $\mathbf{O}_{0:t-1}$ as $[\mathbf{x}_0 = \mathbf{0}, \mathbf{x}_1 = \mathbf{0}, \dots, \mathbf{x}_{t-1} = \mathbf{0}]$ and denote the term

$\mathbf{f}^{\text{dec}}(\mathbf{O}_{0:t-1})$ as $\tilde{\mathbf{h}}_t$. Then, we parameterize a straight line $\gamma(s) : [0, 1] \rightarrow \mathbb{R}^{tD}$ between the actual input $\mathbf{X}_{1:t-1}$ and the input baseline $\mathbf{O}_{0:t-1}$ as

$$\gamma(s) = s\mathbf{X}_{0:t-1} + (1-s)\mathbf{O}_{0:t-1} := [s\mathbf{x}_0, s\mathbf{x}_1, \dots, s\mathbf{x}_{t-1}]. \quad (8)$$

Applying the chain rule in differential calculus, we have

$$\frac{d\mathbf{f}^{\text{dec}}(\gamma(s))}{ds} = \sum_{j=0}^{t-1} \sum_{k=1}^{k=D} \frac{d\mathbf{f}^{\text{dec}}(\gamma_{j,k}(s))}{d\gamma_{j,k}(s)} \frac{d\gamma_{j,k}(s)}{ds} = \sum_{j=0}^{t-1} \sum_{k=1}^{k=D} x_{j,k} \frac{d\mathbf{f}^{\text{dec}}(\gamma_{j,k}(s))}{d\gamma_{j,k}(s)}, \quad (9)$$

where $\gamma_{j,k}(s)$ denote the k -th dimension $s \cdot x_{j,k}$ of the j -th vector $s\mathbf{x}_j$ in point $\gamma(s)$. With the above elements, we can define the below measures.

Definition 3.2 (Dependency Measures). *For an autoregressive decoder \mathbf{f}^{dec} that conditions on both latent variable $\mathbf{x}_0 = \mathbf{z}$ and the prefix $\mathbf{X}_{1:t-1}$ to compute representation \mathbf{h}_t , the dependency measure of every input variable $\mathbf{x}_j, j \in [0, t-1]$ to the decoder is defined as*

$$m_{t,j} = \frac{1}{\|\mathbf{h}_t - \tilde{\mathbf{h}}_t\|^2} \left\langle \mathbf{h}_t - \tilde{\mathbf{h}}_t, \sum_{k=1}^D \left(x_{j,k} \int_0^1 \frac{d\mathbf{f}^{\text{dec}}(\gamma_{j,k}(s))}{d\gamma_{j,k}(s)} ds \right) \right\rangle, \quad (10)$$

where operation $\langle \cdot, \cdot \rangle$ represents the inner product. In particular, we name $m_{t,0}$ as the global dependency and $m_{t,t-j}, 1 \leq j < t$ as the j -th order local dependency.

We provide the derivation for dependency measure $m_{t,j}$ and detail its relations to integrated gradients in Appendix C. In practice, the integral term can be approximated as

$$\int_0^1 \frac{d\mathbf{f}^{\text{dec}}(\gamma_{j,k}(s))}{d\gamma_{j,k}(s)} ds = \mathbb{E}_{s \in \mathcal{U}\{0,1\}} \left[\frac{d\mathbf{f}^{\text{dec}}(\gamma_{j,k}(s))}{d\gamma_{j,k}(s)} \right] \approx \frac{1}{|\mathcal{S}|} \sum_{s \in \mathcal{S}} \frac{d\mathbf{f}^{\text{dec}}(\gamma_{j,k}(s))}{d\gamma_{j,k}(s)}, \quad (11)$$

where \mathcal{S} is the set of independent samples drawn from uniform distribution $\mathcal{U}\{0, 1\}$. According to the law of large numbers [15], this approximation is unbiased and gets more accurate for a bigger sample set $|\mathcal{S}|$. Notably, the defined measures have the following properties.

Proposition 3.3 (Signed and Normalization Properties). *The dependency measure $m_{t,j}, \forall j \in [0, t-1]$ is a signed measure and always satisfies $\sum_{j=0}^{t-1} m_{t,j} = 1$.*

Proof. The proof is fully provided in Appendix D. □

We can see that the measure $m_{t,j}$ can be either positive or negative, with a normalized sum over the subscript j as 1. If $m_{t,j} \geq 0$, then we say that vector \mathbf{x}_j has a positive impact on the decoder \mathbf{f}^{dec} for computing representation \mathbf{h}_j : the bigger is $m_{t,j}$, the larger is such an impact; Similarly, if $m_{t,j} < 0$, then the vector \mathbf{x}_j has a negative impact on the decoder: the smaller is $m_{t,j}$, the greater is the negative influence. Besides, it is also not hard to understand that there exists a negative impact. For example, the latent variable $\mathbf{z} \sim q^{\text{latent}}(\mathbf{z})$ might be an outlier for the decoder \mathbf{f}^{dec} , which locates at a low-density region in the prior distribution $q^{\text{prior}}(\mathbf{z})$.

Example Application. Fig. 1 shows several examples of applying the dependency measures, where each subfigure contains a sample of time series (i.e., blue curve) generated by some model and two types of dependency measures (i.e., red and green bar charts) estimated by Eq. (10). Specifically, every point \mathbf{x}_t in the time series corresponds to a green bar that indicates the global dependency $m_{t,0}$ and a red bar that represents the first-order local dependency $m_{t,t-1}$. For example, in the upper left subfigure, we can see that the positive impact of latent variable \mathbf{z} on the decoder (e.g., $m_{t,0}$) decreases over time and vanishes eventually. From the lower right subfigure, we can even see that some bars (i.e., local dependency $m_{t,t-1}$) are negative, indicating that the variable \mathbf{x}_{t-1} has a negative impact on predicting the next observation \mathbf{x}_t .

Takeaway: Dependency measure $m_{t,j}, 0 \leq j < t$ quantifies the impact of latent variable $\mathbf{x}_0 = \mathbf{z}$ or observation $\mathbf{x}_j, j \geq 1$ on the decoder \mathbf{f}^{dec} . This type of impact can be either positive or negative, which is also reflected in the value of measure $m_{t,j}$.

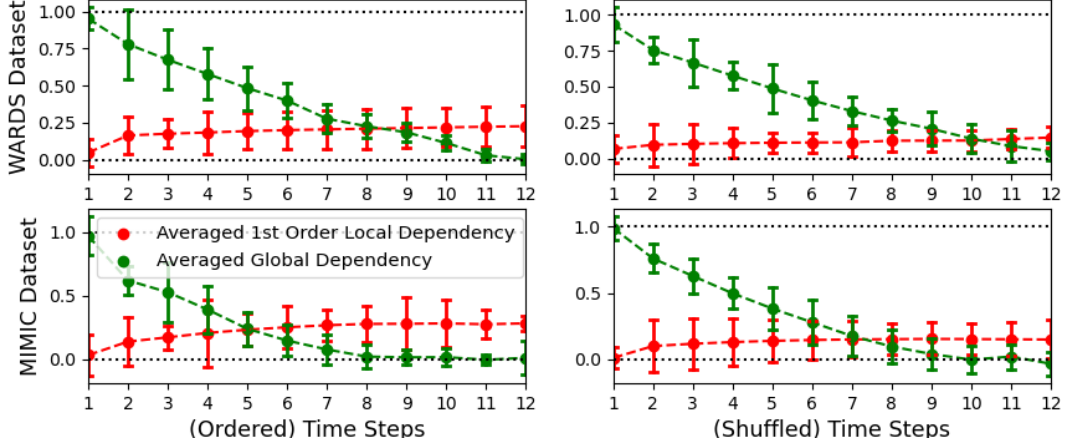


Figure 2: Dependency measures $m_{t,0}, m_{t,t-1}$ averaged over 500 multivariate time series, with 3 standard deviations as the error bars. We can see that the latent variable \mathbf{z} of latent diffusion has a vanishing impact on the decoder \mathbf{f}^{dec} , a typical symptom of *posterior collapse*. We also observe a phenomenon of *dependency illusion* in the case of shuffled time series.

3.3 Empirical Dependency Estimations

We are mainly interested in two types of defined measures: One is the *global dependency* $m_{t,0}$, which estimates the impact of latent variable $\mathbf{x}_0 = \mathbf{z}$ on the decoder \mathbf{f}^{dec} ; The other is the *first-order local dependency* $m_{t,t-1}$, which estimates the dependency of decoder \mathbf{f}^{dec} on the last observation $\mathbf{x}_{t,t-1}$ for computing representation \mathbf{h}_t . In this part, we empirically estimate these measures, with the aims to confirm that *posterior collapse* occurs and show its impacts.

Experiment setup. We adopt two time-series datasets: MIMIC [16] and WARDS [17]. For each dataset, we impute the missing values and extract the observations of the first 12 hours, with the top 1 and 5 features that have the highest variances to form univariate and multivariate time series. To study the case where time series have no structural dependencies, we also try randomly shuffling the time steps of ordered time series. With the prepared datasets, we respectively train latent diffusion models on them and randomly sample time series from the models.

Insightful results. The upper two subfigures of Fig. 1 illustrate the estimated dependencies $m_{t,0}, m_{t,t-1}$ for single time-series sample \mathbf{X} , while Fig. 2 shows the dependency measures averaged over 500 samples. We can see that, for both ordered and shuffled time series, the global dependency $m_{t,0}$ exponentially converges to 0 with increasing time step t , indicating that latent variable \mathbf{z} loses control of the generation process of decoder \mathbf{f}^{dec} and the posterior is *collapsed*. More interestingly, as shown in the right part of Fig. 1, while there is no dependency between adjacent observations $\mathbf{x}_{t-1}, \mathbf{x}_t$ in shuffled time series, we still observe that the first-order measure $m_{t,t-1}$ is significantly different from 0 (e.g., around 0.1 to 0.2). This phenomenon might arise as neural networks overfit and we name it as *dependency illusion*.

Takeaway: Time-series latent diffusion exhibits a typical symptom of *posterior collapse*: latent variable \mathbf{z} has an almost exponentially decreasing impact on generation process $p^{\text{gen}}(\mathbf{X} | \mathbf{z})$. More seriously, we observe a phenomenon of *dependency illusion*.

4 Problem Rethinking and New Framework

In this section, we first analyze the causes of *posterior collapse*, especially in the framework of time-series latent diffusion. Then, in light of our analysis, we propose a new framework, which extends from latent diffusion but addresses the problem.

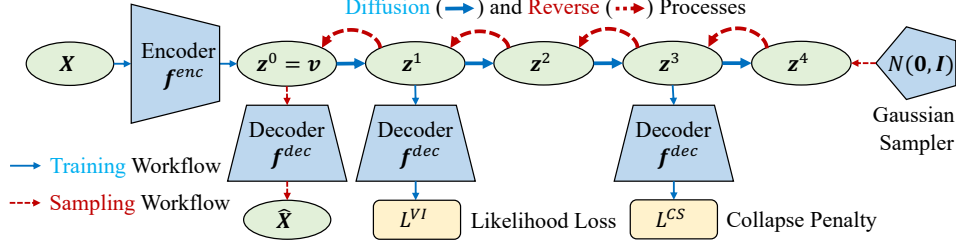


Figure 3: In this example, path $\mathbf{X} \rightarrow \mathbf{z}^1$ is the *variational inference* (which gets rid of KL-divergence regularization) and path $\mathbf{X} \rightarrow \mathbf{z}^3$ shows the *collapse simulation* (which is to increase the sensitivity of decoder f^{dec} to latent variable \mathbf{z}). Compared with time-series latent diffusion, our framework is free from *posterior collapse* and has a unlimited prior $p^{\text{prior}}(\mathbf{z})$.

4.1 Causes of Posterior Collapse

Previous works [18, 19] have identified two main causes of the problem: *KL-divergence term* and *strong decoder*. For time-series latent diffusion, we will explain as below that these causes stem from certain aspects of the framework design.

Over-regularization. The KL-divergence term $D_{\text{KL}}(q^{\text{VI}}(\mathbf{z} | \mathbf{X}) || p^{\text{prior}}(\mathbf{z}))$ in Eq. (2) moves the posterior $q^{\text{VI}}(\mathbf{z} | \mathbf{X})$ towards prior $p^{\text{prior}}(\mathbf{z})$, which has the side effect of *posterior collapse* by definition. In essence, this regularization term is tailored for VAE, such that it is valid to sample latent variable \mathbf{z} from the Gaussian prior $p^{\text{prior}}(\mathbf{z})$ for inference. However, for latent diffusion, the variable \mathbf{z} is sampled from the diffusion model, which can approximate a non-Gaussian prior distribution. Hence, the interaction between the VAE and diffusion model is not properly designed, which incurs a limited prior $p^{\text{prior}}(\mathbf{z})$ and a risky KL-divergence term $D_{\text{KL}}(\cdot)$.

Recurrent time-series decoder. The strong decoder is also a cause of posterior collapse, which happens to the autoencoders for sequence data [3, 20]. Time series $\mathbf{X} \in \mathbb{R}^{TD}$ have a clear temporal structure, so the corresponding decoder f^{dec} is typically a recurrent neural network (RNN) [12], which explicitly models the dependency between different observations $\mathbf{x}_i, \mathbf{x}_j, i \neq j$. For predicting the observation \mathbf{x}_j , both latent variable \mathbf{z} and previous observation $\mathbf{x}_i, i < j$ are the inputs to the decoder f^{dec} , so variable \mathbf{z} is possible to be ignored.

The main difference between time-series and image latent diffusion models is the architecture of decoder f^{dec} . Image decoders (e.g., U-net [21]) are commonly a feedforward neural network (FNN) [22] that contains many layers of CNN [23], self-attention [13], and MLP [24], mapping latent variable \mathbf{z} to the image $\mathbf{X} \in \mathbb{R}^{D \times D}$. Since variable \mathbf{z} is the only input to the image decoder f^{dec} , it is unlikely to be ignored. Indeed, image latent diffusion consistently performs well in practice [1] and is rarely reported with the problem of *posterior collapse*.

Takeaway: The improper design of latent diffusion results in one cause of *posterior collapse*: regularization term $D_{\text{KL}}(\cdot)$, which also limits the form of prior distribution $p^{\text{prior}}(\mathbf{z})$. The recurrent structure of time-series decoder f^{dec} is also a key cause.

4.2 New Framework

In light of previous analyses, we propose a new framework that lets the autoencoder interact with the diffusion model more effectively than latent diffusion: We can get rid of the KL-divergence term and increase the sensitivity of decoder f^{dec} to latent variable \mathbf{z} .

Importantly, we notice a conclusion [2] for the diffusion process (i.e., Eq. (3)):

$$q^{\text{forw}}(\mathbf{z}^i | \mathbf{z}^0) = \mathcal{N}(\mathbf{z}^i; \sqrt{\bar{\alpha}^i} \mathbf{z}^0, (1 - \bar{\alpha}^i) \mathbf{I}), \quad (12)$$

where the coefficient $\bar{\alpha}^i$ monotonically decreases from 1 to approximately 0 for $i \in [0, L]$. In this sense, suppose the initial variable \mathbf{z}^0 is set as $\mathbf{v} = f^{\text{enc}}(\mathbf{X})$, then we can infer that the random variable $\mathbf{z}^i \sim q^{\text{forw}}(\mathbf{z}^i | \mathbf{z}^0)$ contains $\bar{\alpha}^i \times 100\%$ information about the vector \mathbf{v} , with $(1 - \bar{\alpha}^i) \times 100\%$

pure noise. For $i \rightarrow 0$, the diffusion process is similar to the *variational inference* (i.e., Eq. (1)) of VAE, adding slight Gaussian noise to the encoder output \mathbf{v} . For $i \rightarrow T$, the variable \mathbf{z}^i simulates the problem of *posterior collapse* since $q^{\text{forw}}(\mathbf{z}^i | \mathbf{z}^0) \approx \mathcal{N}(\mathbf{z}^i; \mathbf{0}, \mathbf{I})$.

Diffusion process as variational inference. Considering the above facts, we first treat the starting few iterations of the diffusion process as the *variational inference*. Specifically, with a fixed small integer $N \ll L$, we sample a number i from uniform distribution $\mathcal{U}\{0, N\}$ and let the diffusion process convert the encoder output $\mathbf{v} = \mathbf{f}^{\text{enc}}(\mathbf{X})$ into the latent variable:

$$\mathbf{z} = \mathbf{z}^i \sim q^{\text{forw}}(\mathbf{z}^i | \mathbf{z}^0), \mathbf{z}^0 = \mathbf{v}. \quad (13)$$

In terms of the formerly defined generation distribution $p^{\text{gen}}(\mathbf{X} | \mathbf{z})$ (parameterized by the decoder \mathbf{f}^{dec}), a negative log-likelihood loss \mathcal{L}^{VI} is incurred as

$$\mathcal{L}^{\text{VI}} = \mathbb{E}_{i \sim \mathcal{U}\{0, L\}, \mathbf{z}^0} [-\bar{\alpha}^{\gamma i} \ln p^{\text{gen}}(\mathbf{X} | \mathbf{z} = \mathbf{z}^i)], \quad (14)$$

where $\gamma \in \mathbb{N}^+$, $\gamma N \leq L$ is a hyper-parameter, with the aim to reduce the impact of a very noisy latent variable \mathbf{z} . As multiplier γ increases, the weight $\bar{\alpha}^{\gamma i}$ decreases.

Similar to VAE, the variational inference in our framework also leads the latent variable \mathbf{z} to be *smooth* [3] in its effect on decoder \mathbf{f}^{dec} . However, our framework is free from the KL-divergence term $D_{\text{KL}}(q^{\text{VI}}(\mathbf{z} | \mathbf{X}) || p^{\text{prior}}(\mathbf{z}))$ of VAE (i.e., one cause of the *posterior collapse*), since we can facilitate $\mathbf{z} \sim q^{\text{latent}}(\mathbf{z})$ at test time through applying the reverse process of the diffusion model (i.e., Eq. (4)) to sample variable $\mathbf{z}^i, i \in [0, N]$.

Diffusion process for collapse simulation. Then, we apply the last few iterations of the diffusion process to simulate *posterior collapse*, with the purposes of increasing the impact of latent variable \mathbf{z} on conditional generation $p^{\text{gen}}(\mathbf{X} | \mathbf{z})$ and reducing *dependency illusion*.

Following our previous *variational inference*, we set $\mathbf{z}^0 = \mathbf{f}^{\text{enc}}(\mathbf{X})$ and apply the diffusion process to cast the initial variable \mathbf{z}^0 into a highly noisy variable $\mathbf{z}^i, i \rightarrow L$. Considering that the variable \mathbf{z}^i contains little information about the encoder output $\mathbf{f}^{\text{enc}}(\mathbf{X})$, it is unlikely that the decoder \mathbf{f}^{dec} can recover time series \mathbf{X} from variable \mathbf{z}^i , otherwise there is *posterior collapse* or *dependency illusion*. In this sense, we have the following regularization:

$$\mathcal{L}^{\text{CS}} = \mathbb{E}_{i \sim \mathcal{U}\{M, L\}, \mathbf{z}^i} [(1 - \bar{\alpha}^{\lceil \frac{i}{\eta} \rceil}) \ln p^{\text{gen}}(\mathbf{X} | \mathbf{z} = \mathbf{z}^i)], \quad (15)$$

which penalizes the model for having a high conditional density $p^{\text{gen}}(\mathbf{X} | \mathbf{z})$ for non-informative latent variable $\mathbf{z} = \mathbf{z}^i, i \in [M, L]$. Here $M \in \mathbb{N}^+$ is close to L , $\lceil \cdot \rceil$ is the ceiling function, and $\eta \geq 1$ is set to reduce the impact of informative variable \mathbf{z}^i .

For a *strong decoder* \mathbf{f}^{dec} (e.g., LSTM), the regularization \mathcal{L}^{CS} will impose a heavy penalty if the decoder solely relies on previous observations $\{\mathbf{x}_k | k < j\}$ to predict an observation \mathbf{x}_j . In that situation, a high prediction probability will be assigned to the observation \mathbf{x}_j even if the latent variable \mathbf{z} contains very limited information about the raw data \mathbf{X} .

Training and inference. Our framework is similar to latent diffusion for training and inference, with slight differences (e.g., the loss function of autoencoder). We illustrate the workflows of our framework in Fig. 3 and put more details in Appendix E.

5 Experiments

For experiments, we aim to verify that our framework is free from *posterior collapse* and outperforms latent diffusion (with or without previous baselines) in terms of time series generation. Besides presenting the main results as below, we put the details of our experiment setup in Appendix G and the ablation studies in Appendix H.

5.1 Stable Posterior of Our Framework

To show that our framework has a non-collapsed posterior $q^{\text{VI}}(\mathbf{z} | \mathbf{X})$, we follow the same experiment setup (e.g., datasets) as Sec. 3.3 and average the dependency measures $m_{t,0}, m_{t,t-1}$ over 500 sampled

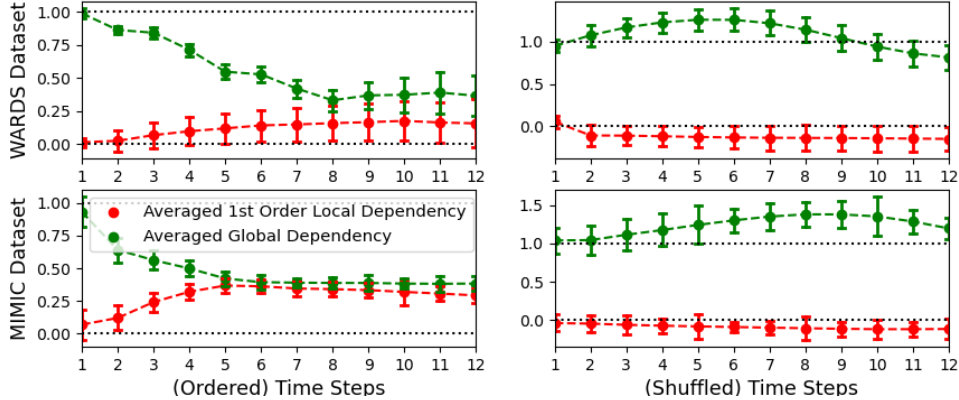


Figure 4: The results of averaged dependency measures and error bars for our framework, which should be compared with those (e.g., Fig. 2) of latent diffusion, showing that our framework has a *stable posterior* and is without *dependency illusion*.

Model	Backbone	MIMIC	WARDS	Earthquakes
Latent Diffusion	LSTM	5.19	7.52	5.87
Latent Diffusion w/ KL Annealing	LSTM	4.28	5.74	3.88
Latent Diffusion w/ Variable Masking	LSTM	4.73	6.01	4.26
Latent Diffusion w/ Skip Connections	LSTM	3.91	4.95	3.74
Our Framework	LSTM	2.29	3.16	2.67
Latent Diffusion	Transformer	5.02	7.46	5.91
Latent Diffusion w/ KL Annealing	Transformer	4.31	5.54	3.51
Latent Diffusion w/ Variable Masking	Transformer	4.42	5.97	4.45
Latent Diffusion w/ Skip Connections	Transformer	3.75	4.67	3.69
Our Framework	Transformer	2.13	3.01	2.49

Table 1: Wasserstein distances [25] of different models on three widely used time-series datasets. The lower the distance metric, the better the generation quality.

time series. The results are illustrated in Fig. 4. For ordered time series in the left two subfigures, we can see that, while the global dependency $m_{t,0}$ still decreases with increasing time step t , it converges into a value around 0.5, which is also a bit higher than the converged first-order local dependency $m_{t,t-1}$. These results indicate that latent variable \mathbf{z} in our framework maintains its control of decoder \mathbf{f}^{dec} during the whole conditional generation process $p^{\text{gen}}(\mathbf{X} | \mathbf{z})$.

For shuffled time series in the right two subfigures, we can see that the global dependency $m_{t,0}$ is always around or above 1, and the local dependency $m_{t,t-1}$ is negative most of the time. These results indicate that the decoder \mathbf{f}^{dec} only relies on latent variable \mathbf{z} and the context \mathbf{x}_{t-1} even has a negative impact on conditional generation $p^{\text{gen}}(\mathbf{X} | \mathbf{z})$, suggesting our framework is without *dependency illusion*. Based on all our findings, we conclude that: compared with latent diffusion (Fig. 2), our framework is free from the effects of posterior collapse (e.g., *strong decoder*).

5.2 Performances in Time Series Generation

In this part, we aim to verify that our framework outperforms latent diffusion in terms of time series generation, which is intuitive since our framework is free from *posterior collapse*. We also include some other methods that are proposed by previous works to mitigate the problem, including KL annealing [26], variable masking [3], and skip connections [27]. We put the details of these baselines in the section of related work: Appendix F.

The experiment results on three commonly used time-series datasets are shown in Table 1. From the results, we can see that, regardless of the used dataset and the backbone of autoencoder, our framework significantly outperforms latent diffusion and the baselines, which strongly confirms our intuition. For example, with the backbone of Transformer, our framework achieves 2.53 points lower than latent diffusion w/ KL Annealing on the WARDS dataset.

References

- [1] Robin Rombach, Andreas Blattmann, Dominik Lorenz, Patrick Esser, and Björn Ommer. High-resolution image synthesis with latent diffusion models. In *Proceedings of the IEEE/CVF Conference on Computer Vision and Pattern Recognition*, pages 10684–10695, 2022.
- [2] Jonathan Ho, Ajay Jain, and Pieter Abbeel. Denoising diffusion probabilistic models. *Advances in Neural Information Processing Systems*, 33:6840–6851, 2020.
- [3] Samuel R. Bowman, Luke Vilnis, Oriol Vinyals, Andrew Dai, Rafal Jozefowicz, and Samy Bengio. Generating sentences from a continuous space. In *Proceedings of the 20th SIGNLL Conference on Computational Natural Language Learning*, pages 10–21, Berlin, Germany, August 2016. Association for Computational Linguistics.
- [4] Pierre Baldi. Autoencoders, unsupervised learning, and deep architectures. In *Proceedings of ICML workshop on unsupervised and transfer learning*, pages 37–49. JMLR Workshop and Conference Proceedings, 2012.
- [5] Diederik P Kingma and Max Welling. Auto-encoding variational bayes. *arXiv preprint arXiv:1312.6114*, 2013.
- [6] Jascha Sohl-Dickstein, Eric Weiss, Niru Maheswaranathan, and Surya Ganguli. Deep unsupervised learning using nonequilibrium thermodynamics. In *International Conference on Machine Learning*, pages 2256–2265. PMLR, 2015.
- [7] David M Blei, Alp Kucukelbir, and Jon D McAuliffe. Variational inference: A review for statisticians. *Journal of the American statistical Association*, 112(518):859–877, 2017.
- [8] Dzmitry Bahdanau, Kyunghyun Cho, and Yoshua Bengio. Neural machine translation by jointly learning to align and translate. *arXiv preprint arXiv:1409.0473*, 2014.
- [9] James Lucas, George Tucker, Roger Grosse, and Mohammad Norouzi. Understanding posterior collapse in generative latent variable models, 2019.
- [10] Prafulla Dhariwal and Alexander Quinn Nichol. Diffusion models beat GANs on image synthesis. In A. Beygelzimer, Y. Dauphin, P. Liang, and J. Wortman Vaughan, editors, *Advances in Neural Information Processing Systems*, 2021.
- [11] Yangming Li, Boris van Breugel, and Mihaela van der Schaar. Soft mixture denoising: Beyond the expressive bottleneck of diffusion models. In *The Twelfth International Conference on Learning Representations*, 2024.
- [12] Sepp Hochreiter and Jürgen Schmidhuber. Long short-term memory. *Neural computation*, 9(8):1735–1780, 1997.
- [13] Ashish Vaswani, Noam Shazeer, Niki Parmar, Jakob Uszkoreit, Llion Jones, Aidan N Gomez, Łukasz Kaiser, and Illia Polosukhin. Attention is all you need. In I. Guyon, U. Von Luxburg, S. Bengio, H. Wallach, R. Fergus, S. Vishwanathan, and R. Garnett, editors, *Advances in Neural Information Processing Systems*, volume 30. Curran Associates, Inc., 2017.
- [14] Mukund Sundararajan, Ankur Taly, and Qiqi Yan. Axiomatic attribution for deep networks. In *International conference on machine learning*, pages 3319–3328. PMLR, 2017.
- [15] Kelly Sedor. The law of large numbers and its applications. *Lakehead University: Thunder Bay, ON, Canada*, 2015.
- [16] Alistair EW Johnson, Tom J Pollard, Lu Shen, Li-wei H Lehman, Mengling Feng, Mohammad Ghassemi, Benjamin Moody, Peter Szolovits, Leo Anthony Celi, and Roger G Mark. Mimic-iii, a freely accessible critical care database. *Scientific data*, 3(1):1–9, 2016.
- [17] Ahmed M Alaa, Jinsung Yoon, Scott Hu, and Mihaela Van der Schaar. Personalized risk scoring for critical care prognosis using mixtures of gaussian processes. *IEEE Transactions on Biomedical Engineering*, 65(1):207–218, 2017.

- [18] Stanislau Semeniuta, Aliaksei Severyn, and Erhardt Barth. A hybrid convolutional variational autoencoder for text generation. In Martha Palmer, Rebecca Hwa, and Sebastian Riedel, editors, *Proceedings of the 2017 Conference on Empirical Methods in Natural Language Processing*, pages 627–637, Copenhagen, Denmark, September 2017. Association for Computational Linguistics.
- [19] Alexander Alemi, Ben Poole, Ian Fischer, Joshua Dillon, Rif A. Saurous, and Kevin Murphy. Fixing a broken ELBO. In Jennifer Dy and Andreas Krause, editors, *Proceedings of the 35th International Conference on Machine Learning*, volume 80 of *Proceedings of Machine Learning Research*, pages 159–168. PMLR, 10–15 Jul 2018.
- [20] Bryan Eikema and Wilker Aziz. Auto-encoding variational neural machine translation. In Isabelle Augenstein, Spandana Gella, Sebastian Ruder, Katharina Kann, Burcu Can, Johannes Welbl, Alexis Conneau, Xiang Ren, and Marek Rei, editors, *Proceedings of the 4th Workshop on Representation Learning for NLP (RepL4NLP-2019)*, pages 124–141, Florence, Italy, August 2019. Association for Computational Linguistics.
- [21] Olaf Ronneberger, Philipp Fischer, and Thomas Brox. U-net: Convolutional networks for biomedical image segmentation. In *Medical image computing and computer-assisted intervention—MICCAI 2015: 18th international conference, Munich, Germany, October 5-9, 2015, proceedings, part III 18*, pages 234–241. Springer, 2015.
- [22] Daniel Svozil, Vladimir Kvasnicka, and Jiri Pospichal. Introduction to multi-layer feed-forward neural networks. *Chemometrics and intelligent laboratory systems*, 39(1):43–62, 1997.
- [23] Alex Krizhevsky, Ilya Sutskever, and Geoffrey E Hinton. Imagenet classification with deep convolutional neural networks. *Advances in neural information processing systems*, 25, 2012.
- [24] Zhou Lu, Hongming Pu, Feicheng Wang, Zhiqiang Hu, and Liwei Wang. The expressive power of neural networks: A view from the width. *Advances in neural information processing systems*, 30, 2017.
- [25] Sebastian Bischoff, Alana Darcher, Michael Deistler, Richard Gao, Franziska Gerken, Manuel Gloeckler, Lisa Haxel, Jaivardhan Kapoor, Janne K Lappalainen, Jakob H Macke, et al. A practical guide to statistical distances for evaluating generative models in science. *arXiv preprint arXiv:2403.12636*, 2024.
- [26] Hao Fu, Chunyuan Li, Xiaodong Liu, Jianfeng Gao, Asli Celikyilmaz, and Lawrence Carin. Cyclical annealing schedule: A simple approach to mitigating KL vanishing. In Jill Burstein, Christy Doran, and Thamar Solorio, editors, *Proceedings of the 2019 Conference of the North American Chapter of the Association for Computational Linguistics: Human Language Technologies, Volume 1 (Long and Short Papers)*, pages 240–250, Minneapolis, Minnesota, June 2019. Association for Computational Linguistics.
- [27] Adji B. Dieng, Yoon Kim, Alexander M. Rush, and David M. Blei. Avoiding latent variable collapse with generative skip models. In Kamalika Chaudhuri and Masashi Sugiyama, editors, *Proceedings of the Twenty-Second International Conference on Artificial Intelligence and Statistics*, volume 89 of *Proceedings of Machine Learning Research*, pages 2397–2405. PMLR, 16–18 Apr 2019.
- [28] Ahmed M. Alaa, Scott Hu, and Mihaela van der Schaar. Learning from clinical judgments: Semi-Markov-modulated marked Hawkes processes for risk prognosis. In Doina Precup and Yee Whye Teh, editors, *Proceedings of the 34th International Conference on Machine Learning*, volume 70 of *Proceedings of Machine Learning Research*, pages 60–69. PMLR, 06–11 Aug 2017.
- [29] U.S. Geological Survey. Earthquake Catalogue (accessed August 21, 2020), 2020.
- [30] Yangming Li. Ts-diffusion: Generating highly complex time series with diffusion models. *arXiv preprint arXiv:2311.03303*, 2023.
- [31] Diederick P Kingma and Jimmy Ba. Adam: A method for stochastic optimization. In *International Conference on Learning Representations (ICLR)*, 2015.

A An Impact of Posterior Collapse

Under the assumption of *posterior collapse*, the below equality:

$$q^{\text{VI}}(\mathbf{z} \mid \mathbf{X}) = p^{\text{prior}}(\mathbf{z}) = \mathcal{N}(\mathbf{z}; \mathbf{0}, \mathbf{I}), \quad (16)$$

holds for any latent variable $\mathbf{z} \in \mathbb{R}^D$ and any conditional $\mathbf{X} \in \mathbb{R}^{TD}$. Then, note that

$$\begin{aligned} q^{\text{latent}}(\mathbf{z}) &= \int q^{\text{VI}}(\mathbf{z} \mid \mathbf{X}) q^{\text{raw}}(\mathbf{X}) d\mathbf{X} = \int \mathcal{N}(\mathbf{z}; \mathbf{0}, \mathbf{I}) q^{\text{raw}}(\mathbf{X}) d\mathbf{X} \\ &= \mathcal{N}(\mathbf{z}; \mathbf{0}, \mathbf{I}) \int q^{\text{raw}}(\mathbf{X}) d\mathbf{X} = \mathcal{N}(\mathbf{z}; \mathbf{0}, \mathbf{I}), \end{aligned} \quad (17)$$

which is exactly our claim.

B Recurrent Encoders

We mainly implement the backbone of decoder \mathbf{f}^{dec} as LSTM [12] or Transformer [13]. In the former case, we apply the latent variable \mathbf{z} to initialize LSTM and condition it on prefix $\mathbf{X}_{1:t-1}$ to compute the representation \mathbf{h}_t . Formally, the LSTM-based decoder \mathbf{f}^{dec} is as

$$\begin{cases} \mathbf{s}_t = \text{LSTM}(\mathbf{s}_{t-1}, \mathbf{x}_{t-1}), \forall t \geq 1 \\ \mathbf{h}_t = \mathbf{W}_f^2 \tanh(\mathbf{W}_f^1 \mathbf{s}_t) \end{cases}, \quad (18)$$

where \mathbf{s}_t is the state vector of LSTM and $\mathbf{W}_f^2, \mathbf{W}_f^1$ are learnable matrices. In particular, for the corner case $t = 1$, we fix $\mathbf{s}_0, \mathbf{x}_0$ as zero vectors.

In the later case, we just treat latent variable \mathbf{z} as \mathbf{x}_0 . Therefore, we have

$$\begin{cases} [\mathbf{s}_{t-1}, \mathbf{s}_{t-2}, \dots, \mathbf{s}_0] = \text{Transformer}(\mathbf{x}_{t-1}, \mathbf{x}_{t-2}, \dots, \mathbf{x}_0) \\ \mathbf{h}_t = \mathbf{W}_f^2 \tanh(\mathbf{W}_f^1 \mathbf{s}_{t-1}) \end{cases}, \quad (19)$$

where the subscript alignment results from self-attention mechanism.

C Derivation of Dependency Measures

Integrated gradient [14] is a very effective method of feature attributions. Our proposed dependency measures can be regarded as its extension to the case of sequence data and vector-valued neural networks. In the following, we provide the derivation of dependency measures.

For the computation $\mathbf{h}_t = \mathbf{f}^{\text{dec}}(\mathbf{X}_{0:t-1})$, suppose the output of decoder \mathbf{f}^{dec} at origin $\mathbf{O}_{0:t-1}$ is $\tilde{\mathbf{h}}_t$, then we apply the fundamental theorem of calculus as

$$\mathbf{h}_t - \tilde{\mathbf{h}}_t = \int_0^1 \frac{d\mathbf{f}^{\text{dec}}(\gamma(s))}{ds} ds, \quad (20)$$

where $\gamma(s)$ is a straight line connecting the origin $\mathbf{O}_{0:t-1}$ and the input $\mathbf{X}_{0:t-1}$ as $\gamma(s) = s\mathbf{X}_{0:t-1} + (1-s)\mathbf{O}_{0:t-1}$. Based on the chain rule, the above equality can be expanded as

$$\begin{aligned} \mathbf{h}_t - \tilde{\mathbf{h}}_t &= \int_0^1 \sum_{j=0}^{t-1} \sum_{k=1}^{k=D} \frac{d\mathbf{f}^{\text{dec}}(\gamma_{j,k}(s))}{d\gamma_{j,k}(s)} \frac{d\gamma_{j,k}(s)}{ds} ds \\ &= \sum_{j=0}^{t-1} \left(\int_0^1 \sum_{k=1}^{k=D} x_{j,k} \frac{d\mathbf{f}^{\text{dec}}(\gamma_{j,k}(s))}{d\gamma_{j,k}(s)} ds \right), \end{aligned} \quad (21)$$

where $\gamma_{j,k}(s)$ denote the k -th dimension $s \cdot x_{j,k}$ of the j -th vector $s\mathbf{x}_j$ in point $\gamma(s)$. Intuitively, every term inside the outer sum operation $\sum_{j=0}^{t-1}$ represents the additive contribution of variable \mathbf{x}_j (to the output difference $\mathbf{h}_t - \tilde{\mathbf{h}}_t$) along the integral line $\gamma(s)$.

Algorithm 1 Autoencoder Training

```

1: repeat
2:   Sample time series  $\mathbf{X}$  from the dataset
3:    $\mathbf{v} = \mathbf{f}^{\text{enc}}(\mathbf{X})$ 
4:    $\mathbf{z}^j \sim q^{\text{forw}}(\mathbf{z}^j | \mathbf{z}^0 = \mathbf{v}), j \sim \mathcal{U}\{0, N\}$ 
5:    $\widehat{\mathcal{L}}^{\text{VI}} = -\bar{\alpha}^{\gamma^j} \ln p^{\text{gen}}(\mathbf{X} | \mathbf{z} = \mathbf{z}^j)$ 
6:    $\mathbf{z}^k \sim q^{\text{forw}}(\mathbf{z}^k | \mathbf{z}^0 = \mathbf{v}), k \sim \mathcal{U}\{M, L\}$ 
7:    $\widehat{\mathcal{L}}^{\text{CS}} = (1 - \bar{\alpha}^{\lceil \frac{k}{n} \rceil}) \ln p^{\text{gen}}(\mathbf{X} | \mathbf{z} = \mathbf{z}^k)$ 
8:   Gradient descent with  $\nabla(\widehat{\mathcal{L}}^{\text{VI}} + \widehat{\mathcal{L}}^{\text{CS}})$ 
9: until converged

```

Algorithm 2 Sampling

```

1:  $\mathbf{z}_L \sim p^{\text{back}}(\mathbf{z}_L) = \mathcal{N}(\mathbf{0}, \mathbf{I})$ 
2:  $i \sim \mathcal{U}\{0, N\}$ 
3: for  $l = L, L-1, \dots, i+1$  do
4:    $\mathbf{z}^{l-1} \sim p^{\text{back}}(\mathbf{z}^{l-1} | \mathbf{z}^l)$ 
5: end for
6: Conditional generation:  $p^{\text{gen}}(\widehat{\mathbf{X}} | \mathbf{z} = \mathbf{z}^i)$ 
7: return Time series  $\widehat{\mathbf{X}}$ 

```

To simplify the notation, we denote the mentioned term as

$$\mathbf{m}_{t,j} = \int_0^1 \sum_{k=1}^{k=D} x_{j,k} \frac{d\mathbf{f}^{\text{dec}}(\gamma_{j,k}(s))}{d\gamma_{j,k}(s)} ds. \quad (22)$$

Since $\mathbf{m}_{t,j}$ is a vector, we map the new term to a scalar and re-scale it as

$$m_{t,j} = \frac{\langle \mathbf{m}_{t,j}, \mathbf{h}_t - \tilde{\mathbf{h}}_t \rangle}{\langle \mathbf{h}_t - \tilde{\mathbf{h}}_t, \mathbf{h}_t - \tilde{\mathbf{h}}_t \rangle}, \quad (23)$$

which is exactly our definition of the dependency measure.

D Properties of of Dependency Measures

Firstly, in terms of Eq. (23), it is obvious that the dependency measure $m_{t,j}$ is signed: the measure can be either positive or negative. Then, based on Eq. (21), we have

$$\mathbf{h}_t - \tilde{\mathbf{h}}_t = \sum_{j=0}^{t-1} \mathbf{m}_{t,j}. \quad (24)$$

By taking an inner product with the vector $\mathbf{h}_t - \tilde{\mathbf{h}}_t$ at both sides, we get

$$\langle \mathbf{h}_t - \tilde{\mathbf{h}}_t, \mathbf{h}_t - \tilde{\mathbf{h}}_t \rangle = \langle \sum_{j=0}^{t-1} \mathbf{m}_{t,j}, \mathbf{h}_t - \tilde{\mathbf{h}}_t \rangle = \sum_{j=0}^{t-1} \langle \mathbf{m}_{t,j}, \mathbf{h}_t - \tilde{\mathbf{h}}_t \rangle. \quad (25)$$

By rearranging the term, we finally arrive at

$$1 = \sum_{j=0}^{t-1} \frac{\langle \mathbf{m}_{t,j}, \mathbf{h}_t - \tilde{\mathbf{h}}_t \rangle}{\langle \mathbf{h}_t - \tilde{\mathbf{h}}_t, \mathbf{h}_t - \tilde{\mathbf{h}}_t \rangle} = \sum_{j=0}^{t-1} m_{t,j}, \quad (26)$$

which is exactly our claim.

E Training and Sampling Algorithms

We present the algorithm of training our autoencoder at Algorithm 1 and the complete inference procedure at Algorithm 2. For the diffusion model in our framework, we train it with the encoder outputs: $\mathbf{v} = \mathbf{f}^{\text{enc}}(\mathbf{X})$, though this is the case for latent diffusion.

F Related Work

While focusing on latent diffusion, our paper is also related to some previous methods that aim to mitigate the problem of *posterior collapse* for VAE [5]. Therefore, we apply three such typical methods to improve the VAE of latent diffusion, with the corresponding experiment results shown in

Table 1. In the following, we briefly introduce those baselines and explain why they cannot match the performance of our framework.

We have included three baselines: latent diffusion w/ KL annealing [3], latent diffusion w/ variable masking [18], and latent diffusion w/ skip connections [27]. For KL annealing, it assigns an adaptive weight to the KL-divergence term, so that VAE is unlikely to fall into the local optimum of posterior collapse at the initial optimization stage. While this method indeed mitigates the problem, but it still does not get rid of the risky KL-divergence regularization. For variable masking (also called decoder weakening), it randomly masks input observations to the autoregressive decoder, such that the decoder is forced to rely more on the latent variable for predicting the next observation. However, this method will make the model less expressive since the decoder is weakened. For skip connections, it directly feeds the latent variable into the decoder at every step, not only at the first step. However, we argue that this method is in fact equivalent to the Transformer-based VAE, where every pairs of input variables to the decoder are also directly connected by self-attention mechanism. In experiments, we find that Transformer-based and LSTM-based latent diffusion are almost the same in terms of their symptoms of posterior collapse. We guess the main reason is that, if the decoder observes the same signal at every time step, it will tend to ignore this seemingly redundant information. There are also many other methods to mitigate the posterior collapse of VAE. For example, cyclical KL annealing [26]. However, they are similar to our adopted baselines, which cannot guarantee that the decoder is sensitive to the latent variable or even are still affected by the risky KL-divergence regularization, with a possibly limited prior distribution.

G Experiment Details

We have adopted three widely used time-series datasets for both analysis and model evaluation, including MIMIC [16], WARDS [28], and Earthquakes [29]. The setup of the first two datasets are introduced in Sec. 3.3. For MIMIC, we specially simplify it into a version of univariate time series for the illustration purpose, which is only used in the experiments shown in Fig. 1. All other experiments are about multivariate time series. For the Earthquakes dataset, it is about the location and time of all earthquakes in Japan from 1990 to 2020 with magnitude of at least 2.5 from [29]. We follow the same preprocessing procedure for this dataset as [30].

We use almost the same model configurations for all experiments. The diffusion models are parameterized by a standard U-net [21], with $L = 1000$ diffusion iterations and hidden dimensions $\{128, 64, 32\}$. The hidden dimensions of autoencoders and latent variables are fixed as 128. The conditional distribution $p^{\text{gen}}(\mathbf{X} | \mathbf{z})$ is parameterized as a Gaussian, with learnable mean vector and diagonal covariance matrix functions. For our framework, N, M are respectively selected as 50, 100, with $\gamma = 2$ and $\eta = 1$. We also apply dropout with a ratio of 0.1 to most layers of neural networks. We adopt Adam algorithm [31] with the default hyper-parameter setting to optimize our model. For Table 1 and Table 2, every number is averaged over 10 different random seeds, with a standard deviation less than 0.05. For the computing resources, all our models can be trained on 1 NVIDIA Tesla V100 GPU within 10 hours.

H Ablation Studies

We have conducted ablation studies to verify that our hyper-parameter selections $N = 50, M = 100$ are optimal. The experiment results are shown in Table 2. For both N and M , either increasing or decreasing their values results in worse performance on the two datasets.

I Conclusion

In this paper, we provide a solid analysis of the negative impacts of *posterior collapse* on time-series latent diffusion and introduce a new framework that is free from this problem. For our analysis, we begin with a theoretical insight, showing that the problem will reduce latent diffusion to VAE, making it *less expressive*. Then, we introduce a useful tool: *dependency measures*, which quantify the impacts of various inputs on an autoregressive decoder. Through empirical dependency estimation, we show that the latent variable has a vanishing impact on the decoder and find that latent diffusion exhibits a phenomenon of *dependency illusion*. Compared with standard latent diffusion, our framework gets

Model	Backbone	N for \mathcal{L}^{VI}	M for \mathcal{L}^{CS}	Diffusion Iterations L	MIMIC	WARDS
Latent Diffusion	Transformer	–	–	1000	5.02	7.46
LD w/ Skip Connections	Transformer	–	–	1000	3.75	4.67
Our Framework	Transformer	50	100	1000	2.13	3.01
Our Framework	Transformer	50	50	1000	2.59	3.32
Our Framework	Transformer	50	150	1000	2.71	3.46
Our Framework	Transformer	50	200	1000	2.83	3.75
Our Framework	Transformer	10	100	1000	2.31	3.16
Our Framework	Transformer	100	100	1000	2.38	3.24
Our Framework	Transformer	150	100	1000	2.75	3.41

Table 2: Ablation studies of the hyper-parameters N , M , which are respectively used in the estimations of likelihood loss \mathcal{L}^{VI} and collapse penalty \mathcal{L}^{CS} . Here LD is short for latent diffusion and the symbol – means “Not Applicable”.

rid of the risky KL-divergence regularization, permits an unlimited prior distribution, and lets the decoder be sensitive to the latent variable. Extensive experiments on multiple real-world time-series datasets show that our framework has no symptoms of posterior collapse and notably outperforms the baselines in terms of time series generation.